



# Late Ediacaran magnetostratigraphy of Baltica: Evidence for Magnetic Field Hyperactivity?



Mikhail L. Bazhenov<sup>a,b,\*</sup>, Natalia M. Levashova<sup>a</sup>, Joseph G. Meert<sup>c</sup>, Inessa V. Golovanova<sup>d</sup>, Konstantin N. Danukalov<sup>d</sup>, Natalia M. Fedorova<sup>a</sup>

<sup>a</sup> Geological Institute, Russian Academy of Sciences, Moscow, Russia

<sup>b</sup> Institute of Physics of the Earth, Russian Academy of Sciences, Moscow, Russia

<sup>c</sup> Department of Geological Sciences, University of Florida, Gainesville, FL, USA

<sup>d</sup> Institute of Geology, Ufa Scientific Center, Russian Academy of Sciences, Ufa, 450000 Russia

## ARTICLE INFO

### Article history:

Received 17 December 2014

Received in revised form 27 October 2015

Accepted 16 December 2015

Available online 31 December 2015

Editor: G.M. Henderson

### Keywords:

Baltica  
Late Ediacaran  
paleomagnetism  
magnetostratigraphy  
ultra-high reversal rate

## ABSTRACT

Long-term changes in characteristics of the geomagnetic field may signal evolutionary changes within the Earth's interior. Among these long-term variations, the magnetic field reversal rate is probably the best known and most frequently used parameter to evaluate concomitant changes in the Earth's core. Although the reversal rate is well known for the last 150 Ma and reasonably constrained back to 300 Ma, knowledge of the early Paleozoic and earlier times is limited. Hence, the haunting question is whether the reversal pattern for the last 300 Myr is a good representation of the field behavior over a much longer interval. A paleomagnetic study of Upper Ediacaran sediments from the Zigan Fm. (Baltica in the western South Urals) revealed a high-temperature, dual-polarity component that is of primary origin (Levashova et al., 2013). In this paper, we present the results of a magnetostratigraphic study from the same sections that can be summed up as follows: 1) >30 magnetozone are found in the ca. 110 meters thick composite section of the Zigan Fm.; 2) A similar reversal pattern was reported from Upper Ediacaran sediments from the White Sea coast (North Russia) and SW Siberia but has never been found in clastic rocks of any other age; 3) The reversal pattern in three remote Ediacaran sections could not result from remagnetization or extremely slow sedimentation; 4) The reversal rate in the Late Ediacaran exceeded 20 reversals per million years; 5) The field appears to behave in a bipolar fashion during the period of hyperactivity.

© 2015 Elsevier B.V. All rights reserved.

## 1. Introduction

More than a millennium ago, humans discovered the existence of the geomagnetic field. Several centuries ago, it became clear that the magnetic field does not have a random structure and less than a century ago we understood that the field has not remained in a single polarity state. A few decades ago, scientists discovered that the pattern of magnetic field reversals forms a complex series. Two major questions now haunt the geo- and paleomagnetic communities: What is the structure of this series, otherwise known as the magnetostratigraphic scale? What does this structure mean?

\* Corresponding author at: Geological Institute, Russian Academy of Sciences, Moscow, Russia.

E-mail addresses: mibazh@mail.ru (M.L. Bazhenov), namile2007@rambler.ru (N.M. Levashova), jmeert@ufl.edu (J.G. Meert), golovanova@anrb.ru (I.V. Golovanova), danukalov@mail.ru (K.N. Danukalov), namife90@gmail.com (N.M. Fedorova).

The reversal pattern for the most recent 150 Myr is well known due, in large part, to the analysis of seafloor magnetic anomalies paired with magnetostratigraphic studies on land. Deeper in geologic time (back to about 300 Ma), magnetostratigraphic data obtained from sedimentary sections are patchier, but still allow a general pattern to emerge. For still older times, data may be absent for many tens of Myr, and often the only conclusion that can be reached is “There were reversals”, or “There were no reversals”. Nevertheless, the available data show that the geomagnetic reversal frequency has varied significantly over time, from the zero value during superchrons to epochs, when 7–8, perhaps up to ten, reversals could occur for one million years (Opdyke and Channell, 1996; Biggin et al., 2012; Pavlov and Gallet, 2005, 2010).

Of particular interest is the question of whether the reversal scale for the last 300 Myr is a good representation of field behavior over a much longer interval. In particular, it is important to find out, whether the rate of about 7–8 RMa<sup>−1</sup> (reversals per million years) in the Middle Jurassic provides an upper bound on reversal frequency (Biggin et al., 2012).

With different aims in mind, [Levashova et al. \(2013\)](#) carried out a study on about 400 samples of greenish-gray and maroon clastics of the Upper Ediacaran Zigan Formation from the westernmost part of the South Urals, which is the deformed margin of cratonic Baltica. The main conclusions can be summed up as follows: 1) Above 200 °C to 300 °C, a single high-temperature component, HTC, showing rectilinear decay to the origin is present in most samples of reddish varieties. 2) The shallow HTC has dual-polarity and is most likely primary, with most unit vectors falling into polarity groups with east–southeast or west–northwest declinations; the reversal test for these data is positive. 3) No large inclination shallowing had affected this HTC. 4) Analysis of geological data and late Paleozoic overprint directions from the western parts of the South Urals indicates that the study area was neither noticeably displaced nor rotated with respect to Baltica. 5) Finally, by comparison with coeval poles from Laurentia, it was found that the paleomagnetic directions with east–southeast declinations (and paleomagnetic poles near Australia) are likely to correspond to normal polarity. Hence the Uralian margin of Baltica faced north and was at a paleolatitude of ca. 10°S in Late Ediacaran time.

Although not discussed in detail, it was found that the samples with opposite HTC polarities in a section are often separated by several decimeters to a few meters. We present the polarity pattern in the Zigan rocks in more detail in this paper and discuss possible implications.

## 2. Geological setting and sampling

The Ural fold belt is a composite fold-thrust belt, and tectonic units of its eastern half are allochthonous with respect to Baltica and docked with it in the Devonian and Late Paleozoic ([Puchkov, 2003](#); [Brown et al., 2006](#)). In contrast, the western parts of the fold belt show similarities to cratonic Baltica ([Puchkov, 1997, 2003](#); [Levashova et al., 2013](#); [Kuznetsov et al., 2014](#)). In particular, a more than ten kilometers thick succession of Meso- and Neoproterozoic clastic sediments and carbonates with subordinate Mesoproterozoic volcanics ([Keller and Chumakov, 1983](#)) is exposed in the Bashkir Anticlinorium (Uplift) in the western South Urals ([Fig. 1a–b](#)). Geological and geophysical data indicate that this area was a part of the Baltica deformed margin at least since the early Neoproterozoic (~1 Ga; [Puchkov, 2003](#)).

The uppermost member of this succession, the Asha Series, contains up to two km thick terrigenous clastics ([Keller and Chumakov, 1983](#); [Bekker, 1988](#)). The Asha Series clastics paraconformably (and locally unconformably) overlie earlier Neoproterozoic rocks and are paraconformably overlain by Middle Ordovician sediments in the south and Lower Devonian (Emsian) sandstone elsewhere. There are no angular unconformities between the base of the Asha Series and mid-Permian rocks to the west of the Zilmerdak Fault (thick red line in [Fig. 1b](#)), and the only folding event in the westernmost Urals took place in mid-Permian time (Kungurian, 270–275 Ma; [Puchkov, 2003](#)).

The Asha Series is divided, in ascending order, into the Bakeev, Uryuk, Basu, Kuk-Karauk and Zigan Formations ([Figs. 1c, 2b](#)). The two older units are predominately arkoses, whereas the younger three are polymictic. Sandstone and siltstone, with subordinate mudstone and rare gritstone, prevail through the Asha Series. The only conglomerate in the Series is in the Kuk-Karauk Fm.; this conglomerate member is up to 50 m thick in the south but thins out to a few meters in the center of the area and wedges out in the north. The uppermost member of the Series, the Zigan Fm., comprises up to 450 meters, usually ~300 meters, of greenish-gray and brown-gray, sometimes maroon, fine-grained sandstone with subordinate siltstone. Its contact with the underlying Kuk-Karauk Fm. is reportedly gradual but, to our knowledge, has never been

observed in a continuous exposure. Interbedded sandstone and siltstone of the Zigan Fm. accumulated in shallow basin with sedimentary fill generally wedging out westward. Together with the two underlying formations, the Zigan Fm. is regarded as molasse ([Bekker, 1988](#)), with the sediment transport from the east. This is confirmed by a study of detrital zircons provenance that revealed zircon grains with Baltica typical ages but found a large share of 1.0–1.5 Ga old zircons that are “alien” to the eastern part of the craton ([Kuznetsov et al., 2012, 2014](#)).

Generally, sandstones are more abundant in the Basu Fm. and siltstones prevail in the Zigan Fm., but both varieties are common in these formations. As just minor parts of both formations are present at most outcrops, whereas the complete sections with exposed top and bottom are absent, it is often difficult to distinguish Basu from Zigan. The distinction between the two formations is almost entirely based on the clearly recognizable and often well exposed Kuk-Karauk conglomerate. This identification, however, becomes contestable in the northernmost part of the Bashkir Uplift, where the Kuk-Karauk conglomerate is absent. In spite of this difficulty, paleomagnetic directions from the Basu and Zigan Formations show distinct signatures ([Levashova et al., 2013, 2015](#)) and may aid in future attempts to delineate the stratigraphic relationships in the region.

Until recently, no volcanic rocks were known in the Asha Series; hence, no isotopic age determinations were available. Then, several thin (<10 cm) tuff layers were found among Ediacaran rocks in the Ust-Katav section the northernmost part of the Bashkir Uplift (blue square, UK, in [Fig. 1b](#); [Grazhdankin et al., 2011](#)). Here, the Ediacaran rocks are represented by siltstones with thin layers of fine-grained sandstones and were originally regarded as the upper part of the Zigan Fm. ([Grazhdankin et al., 2011](#)). Several thin tuff layers within an about five meters thick interval were found some 80 m below the disconformable contact between Ediacaran rocks and sandstones of the Emsian Takata Fm. The reported U–Pb age on zircons (LA-IPC-MS) from one of these tuff beds is  $547.6 \pm 3.8$  Ma ([Levashova et al., 2013](#)). The Kuk-Karauk conglomerate is absent in UK area and thus it is unclear whether the dated tuff belongs to the Zigan or Basu Fm. In more recent papers ([Grazhdankin, 2014](#); [Kolesnikov et al., 2015](#)), the dated tuff was ‘relocated’ to the Basu Fm. and the upper four formations of the Asha series are regarded as younger than 550 Ma. We do not think that the age problems of this Series are all settled, but further discussion is out of scope of this paper. The Kuk-Karauk conglomerate is present in the South Urals, and the recognition of the Zigan Fm. is unambiguous. In 2011, a tuff layer at the very top of the exposed section and three tuff layers within a three meters interval among the redbeds of the Zigan Fm. that were sampled for a paleomagnetic study were found among the Zigan rocks (section Z4 in [Fig. 1b](#); [Fig. 2a](#); [Levashova et al., 2013](#)). Unfortunately, just a few rounded zircon grains yielded disparate ages of >600 Ma were found in three layers. Still, the presence of multiple tuff beds within the narrow stratigraphic intervals and geological evidence let [Levashova et al. \(2013\)](#) attribute the age of ~ about 545–550 Ma to the Zigan rocks.

The sampled sections of the Zigan Fm. numbered Z1 to Z4 ([Fig. 1b](#)) have similar gentle dips to the west. Most samples are finely laminated fine-grained silty sandstones that were collected as blocks oriented with a magnetic compass and later cut into cubic specimens. In advance, we would like to note that brown-red rocks were sampled over the entire exposed intervals at sections Z1, Z3 and Z4. A large collection (>100 samples) of greenish-gray varieties from the upper larger part of the Zigan Fm. ([Fig. 2b](#)) did not yield interpretable data and is not used further on (for more detail, see [Levashova et al., 2013](#)).

At locality Z1, a ~30 meter thick continuous exposure of red, brown and greenish-gray sandstones was sampled from a road cut.

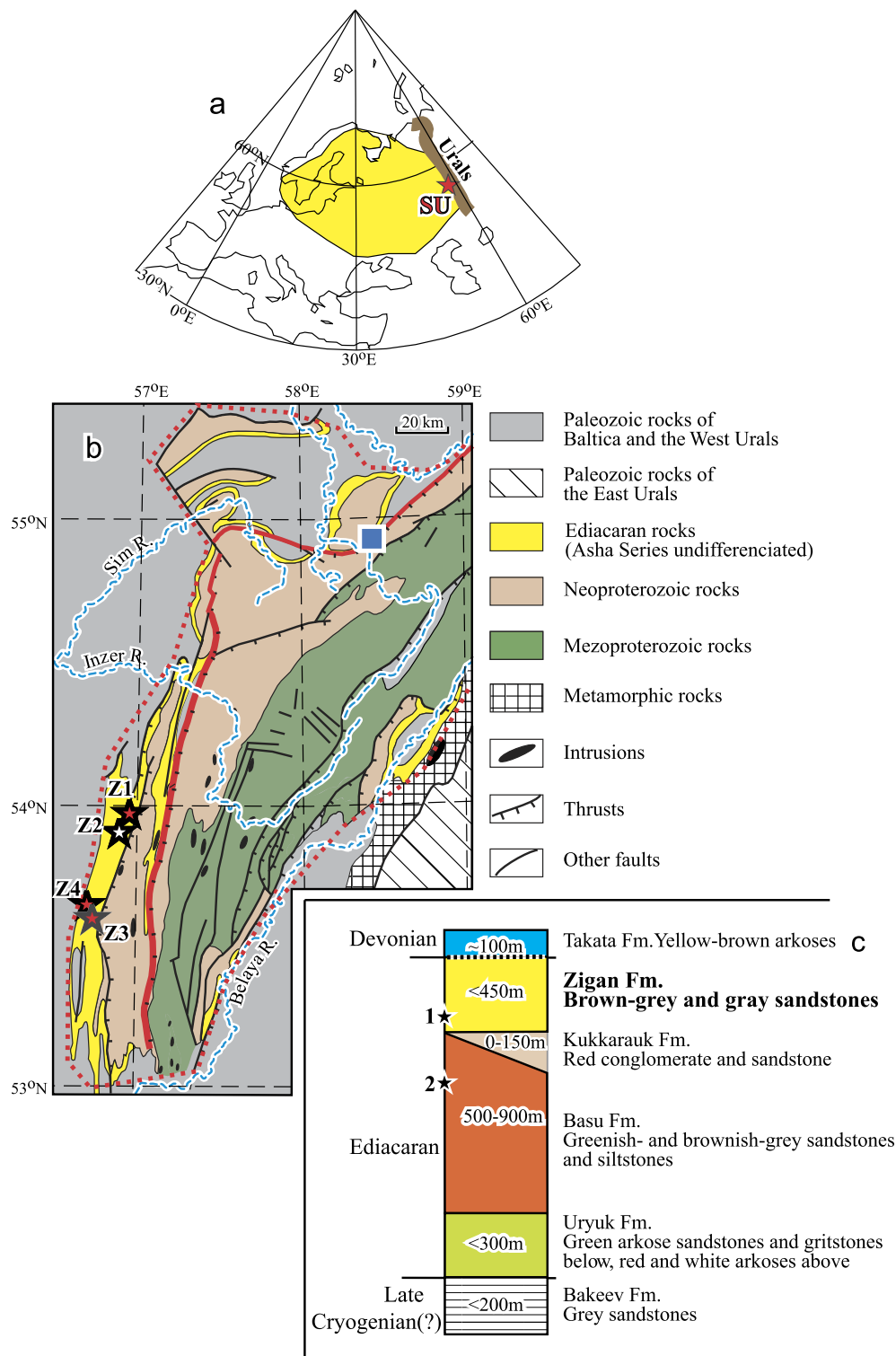


**Fig. 1.** (a) Location of the Baltica block with Precambrian basement (shaded), the Urals (brown band) and the study area in the South Urals (SU, red star). (b) Schematic map of the SW Urals with the limits of the Bashkir Uplift shown as thick dotted line (simplified after Kozlov, 2002). The thickest red line denotes the Zilmerdak Fault, to the west of which Ediacaran rocks are overlain by Paleozoic rocks without angular unconformity. Stars denote the sections numbered as in Section 2 and Table 1, where the Upper Ediacaran Zigan Formation was sampled (discarded section Z2 is shown by open star). Square denotes the locality where U–Pb age was determined (Grazhdankin et al., 2011). (c) Schematic stratigraphic column of the Ediacaran sequence (Asha Series) of the SW Urals. Thick dashed line denotes stratigraphic unconformity between Ediacaran and Paleozoic rocks. Stars denote the inferred positions of the dated tuff bed: 1, according to Grazhdankin et al. (2011) and Levashova et al. (2013); 2, according to Grazhdankin (2014) and Kolesnikov et al. (2015); see Section 4 for discussion. (For interpretation of the references to color in this figure legend, the reader is referred to the web version of this article.)

The exposure base is about 20 meters above the Kuk-Karauk conglomerate, which is about four meter thick here. The lower three meters of the section comprise brown- to brick-red fine grained sandstone (8 samples) that is succeeded by ca. 8–9 meters thick

very fine-grained maroon sandstone and siltstone (23 samples in total).

At section Z3, the about 30 meters thick Kuk-Karauk conglomerate is exposed on the right side of the Zigan River valley. An

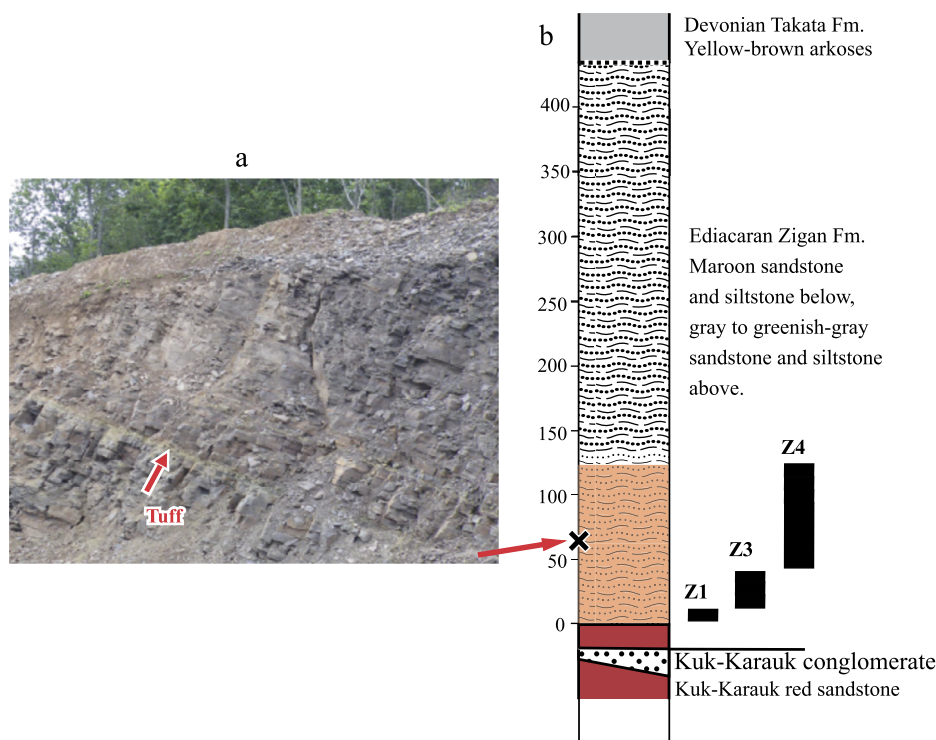


**Fig. 2.** (a) Exposure of Zigan red beds at section Z4 (view to the southwest). (b) The upper part of the same stratigraphic column as in Fig. 1c and approximate location of the studied Zigan sections labeled as in Section 2 and Fig. 1b. Thick dashed line denotes stratigraphic unconformity between Ediacaran and Paleozoic rocks. The position of the tuff bed that we could NOT date is shown as oblique cross. (For interpretation of the references to color in this figure legend, the reader is referred to the web version of this article.)

interval of about 30 meters is not exposed, and, after it, a nearly continuous outcrop begins on the left side of the valley. Its lower half (35–40 meter thick) comprises fine- to medium-grained maroon and brown-gray sandstones, from which 69 samples were collected, with 0.5 m distance between them, on average.

Finally, at section Z4 that is ~three kilometers to the north from the Z3 section, a several meters thick section of the Kuk-Karauk conglomerate is exposed in a fresh road cut. Then, this road crosses a deep ravine without exposures; the missing part of the section is 50–60 meter thick. On the other side of the ravine, the outcrop along the same deep road cut begins with a few meter thick greenish sandstones (not sampled) that are succeeded with an about 80 meter thick pile of brown to red sandstones (Fig. 2a) with several one to three meter-thick greenish beds. With a rather sharp transition, the redbeds are overlain with about 200 meters thick greenish sandstone and siltstone sequence that was not sampled. 127 samples were spread more or less uniformly over the 80-meter thick redbed member.

In 2011, one hand-sized block per stratigraphic level was taken from three main sections (Z1, Z3 and Z4), sampling points being spaced by 0.5 meter on average. The samples were arranged in stratigraphic order at each section using measured thicknesses and the distance from the top of the Kuk-Karauk conglomerate (Fig. 2b). The studied parts of sections Z1 and Z3 do not overlap, but the distance in meters between the top Z1 and bottom Z3 is difficult to establish, but is unlikely to be >20 m. The top Z3 and the base Z4 may slightly (i.e., by a few meters) overlap or be on a similar level (Fig. 2b). With reservations that are clear from the preceding description, we conclude that the total studied interval slightly exceeds 100 meters. This collection served as a base for tectonic interpretation of paleomagnetic data (Levashova et al., 2013); the same collection is used for determination of the reversal rate and geomagnetic field characteristics and magnetostratigraphy

that is presented in this paper. In 2014, eight different thin beds, each <10 cm thick and from five to eight meters in length, were sampled at section Z4 to evaluate the within-bed scatter of paleomagnetic directions and to get an estimate of the secular variation, SV, magnitude (Merrill et al., 1996). Note that the samples from the thin-bed sites were not included into calculation of the overall mean and related statistics.

### 3. Paleomagnetism

#### 3.1. Methods

A cubic specimen of 8-cm<sup>3</sup> volume from each sample was studied in the Paleomagnetic Laboratories of Geological Institute of the Russian Academy of Sciences in Moscow and of Institute of Geology of the Uralian Branch of the Russian Academy of Sciences in the Ufa City. Individual specimens were stepwise heated in 12 to 20 increments up to 700 °C in either homemade ovens (Moscow) or utilizing an Analytical Services TD-48 thermal demagnetizer with internal residual fields of <10 nT (Ufa); measurements were done with a JR-4 or JR-6 spinner magnetometer with a noise level of 0.05 mA/m. Sister-specimens from ~20% of the collection were demagnetized in both laboratories and showed good consistency, most isolated components agreeing within 10°. Demagnetization results were plotted in orthogonal vector diagrams (Zijderveld, 1967). Visually identified linear trajectories were used to determine directions of magnetic components by Principal Component Analysis (PCA), employing a least-squares fit comprising three or more demagnetization steps (Kirschvink, 1980). Statistics at the sample level was used for calculation of the section-mean and overall mean directions. PaleoMac software (Cogné, 2003) was used in the analysis.



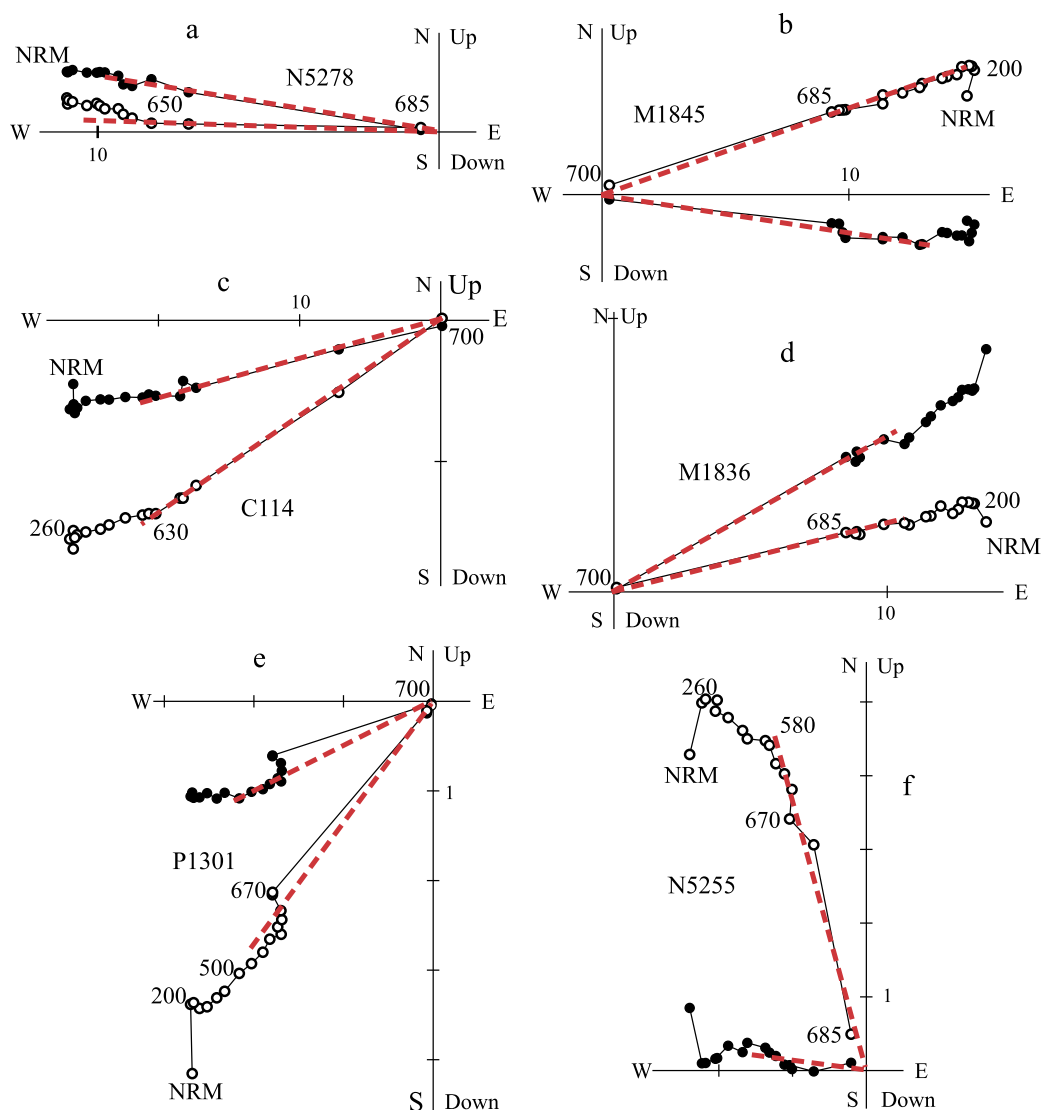


**Fig. 3.** Representative thermal demagnetization plots of brown-gray and maroon fine-grained sandstones and siltstones of the Ediacaran Zigan Formation from the western part of the South Urals, in stratigraphic coordinates. a–d, samples with HTC directions in the main polarity groups, e–f, samples with anomalous HTC directions. Isolated high-temperature components are denoted by thick red dashed lines. Temperature steps are in degrees Celsius. Magnetization intensities are in mA/m. Full (open) circles represent vector endpoints projected onto the horizontal (vertical) plane. (For interpretation of the references to color in this figure legend, the reader is referred to the web version of this article.)

### 3.2. Results

The data acquisition was described in detail by Levashova et al. (2013) and is briefly presented here. After removal of a weak unstable remanence below 200° to 300°, a high-temperature component (HTC) showing rectilinear decay to the origin is isolated from most samples of maroon sandstones and siltstones (Fig. 3); no samples with demagnetization trajectories bypassing the origin were found. Final components for ~25 pilot samples from the main collection and all samples from the thin-bed sites were calculated with anchoring the fitting lines to the origin where appropriate and without this. Mean directions for these two approaches are found to agree within 2–3°, but the “anchored” data proved to be less dispersed; consequently, all results below are based on such data. In some samples, the HTC is preceded by an intermediate-temperature component that accounts for a minor part of the total magnetization; this remanence with nearly chaotic directions is likely a mixture of the present-day overprint and HTC (Fig. 3c, f). Most HTC vectors form distinct polarity groups with east-southeast or west-northwest declinations (Fig. 4a). The

reversal test (McFadden and McElhinny, 1990) is positive at the site level ( $n = 36$  sites):  $\gamma = 5.7^\circ < \gamma_0 = 9.9^\circ$ , where  $\gamma$  is the observed angle between the polarity-means, and  $\gamma_0$  is the critical angle at the 95% significance level. Unexpectedly, the outcome of the test changes at the sample level: while  $\gamma_0$  decreases to  $6.4^\circ$ ,  $\gamma$  increases to  $8.1^\circ$ . We cannot account for this result but think that it is still possible to speak about a (nearly) perfect antipodality of polarity-mean directions. The fold test is inconclusive because of very similar bedding attitudes in all sections of the Zigan redbeds (Table 1). The Zigan pole at  $PLat = 138^\circ N$ ,  $PLong = 16^\circ E$  ( $A_{95} = 4^\circ$ ) is far away from the Phanerozoic apparent polar wander path for Baltica (Torsvik et al., 2012) but agrees with nearly coeval late Ediacaran data from the White Sea part of the craton (Popov et al., 2002, 2005; Iglesia Llanos et al., 2005). This as well as the presence of a dual-polarity remanence is strong indication of a primary origin of the HTC for the Zigan rocks.

The HTC sample directions in the Zigan rocks give a precision parameter  $k$  value of 11.6 (Fig. 4) that is the total dispersion  $k_t$  and is in turn the sum of the within-site  $k_{ws}$  and between-site  $k_{bs}$  dispersions (Merrill et al., 1996); similar relationship is valid for VGPs

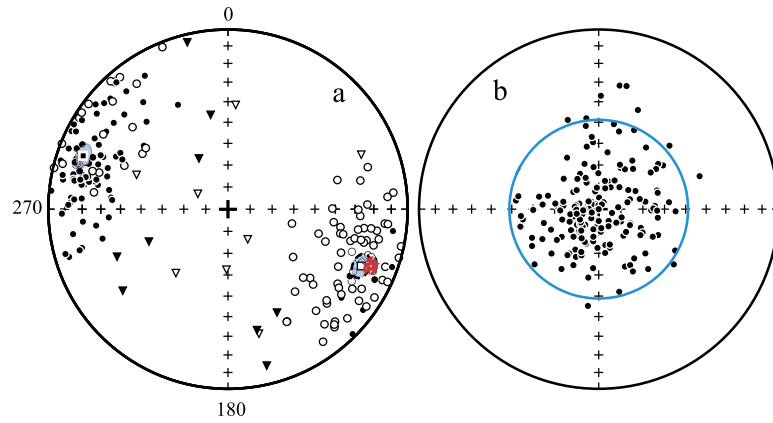


**Fig. 4.** Equal-area projections of high-temperature components for all three sections combined. (a) Tilt-corrected steady-field directions from main polarity groups (circles), the polarity means (squares) and the overall mean (red star) with associated confidence circles and anomalous directions (inverted triangles). (b) Steady-field directions inverted to one polarity with the mean direction transferred to the stereonet pole. Blue circle is for better evaluation of the distribution form. (For interpretation of the references to color in this figure legend, the reader is referred to the web version of this article.)

**Table 1**

Summary of paleomagnetic results from the Zigan Fm.

Section	TH	Strike °	Dip °	<i>n</i>	D°	I°	<i>k</i>	$\alpha_{95}^{\circ}$	PZ
Z1	8–9	204	22	23/22/1	106.4	–15.5	12	9.4	7(1)
Z3	35–40	195	25	69/59/8	114.0	–11.3	10	6.1	17(3)
Z4	75–80	208	23	125/101/9	111.6	–17.9	13	4.1	19(1)
Samples	~100	–	–	217/182	111.7	–15.5	12	3.2	>30?
Samples*	~100	–	–	217/182	111.5	–23.3	8	3.9	–
Sites**	~100	–	–	(36)	106.5	–15.6	26	4.8	–

Comments. Sections are labeled as in Section 2 and Fig. 1b. Samples (sites) are the overall means for the steady-state data only. Strike and dip are average bedding attitudes of the sampled sections. TH is the true thickness of the sections in meters. *n* is the number of samples (sites) studied/steady-state HTC directions/anomalous directions (see Section 3.2 for more detail). D, I, are mean declination and inclination in stratigraphic coordinates. *k* is concentration parameter.  $\alpha_{95}$  is radius of confidence circle (Fisher, 1953). PZ is the number of polarity zones (those based on single samples).

\* Same dataset but corrected for inclination shallowing with  $f = 0.6$ .

\*\* Taken from Levashova et al. (2013).

**Table 2**

HTC data from thin-bed sites.

Site	Strike °	Dip °	<i>n</i>	In situ				Tilt-corrected			
				D°	I°	<i>k</i>	$\alpha_{95}^{\circ}$	D°	I°	<i>k</i>	$\alpha_{95}^{\circ}$
M3551	181	26	9/9	111.4	–33.7	73.2	6.1	108.2	–9.1	78.1	5.9
M3560	201	23	9/9	122.7	–42.1	56.7	6.9	120.2	–19.6	73.5	6.0
M3580	191	22	8/7	262.6	47.6	48.8	8.7	267.1	26.2	48.8	8.7
M3570	180	24	10/0	No stable remanence							
F0630	204	24	9/9	292.1	39.0	44.7	7.8	292.5	15.2	39.1	8.3
F0639	202	24	9/9	275.2	37.8	36.4	8.6	278.3	14.4	34.8	8.9
F0657	196	26	7/6	122.0	–50.9	18.0	16.2	117.0	–25.5	23.3	14.2
F0648*	204	20	9/5	291.9	–7.5	10.5	24.7	291.7	–28.0	10.9	24.3

Sites are presented in stratigraphic order, site F0648 being the lowest. *n* is the number of samples studied/accepted for calculation of site-means. Other notation as in Table 1.

\* Excluded from analysis because of large data scatter.

too. Of eight thin-bed sites, no stable remanence was isolated at site M3570, and few scattered HTC directions do not decay to the origin at site F0648, which was discarded too. Of the remaining six sites, three have one polarity and three the other, the corresponding site-means being nearly antipodal and concentration parameter values  $k_{ws}$  ranging from 23 to 78, ~50 on average (Table 2). Taking the latter value as an estimate of the within-site scatter  $k_{ws}$  leads to  $k_{bs} = 11.9$  that differs from the original value by <3%. For VGPs, the “removal” of the within-site scatter changes  $K_t$  by similar amount too. One polarity only was found at each thin-bed site, and these data strongly indicate the strata-bound character of remanence in the Zigan rocks.

The distribution of HTC directions is weakly elongated (Fig. 4b), the observed elongation  $E = 1.36$  being much less than  $E$  values of 2.6–2.8 predicted for the observed paleolatitude of ca. 10° by most field models (Tauxe and Kent, 2004; Tauxe et al., 2008). With

the aid of the elongation/inclination method (ibid.), the flattening factor  $f$  is found to be ~0.6 for the Zigan collection, which corresponds to inclination shallowing by ~8° (L. Tauxe, written communication, 2015); note that unflattening has also resulted in noticeable increase in dispersion, from  $k = 12$  to  $k = 8$  (Table 1). We do not think, however, that the above correction is uncontested. First, the observed cloud of directions (Fig. 4a) is the sum of SV-related elongated distribution and a Fisher-like distribution because of within-site scatter. As a result, their superposition will be more circular than predicted by field models. Secondly, the variance of elongation values is large even for simulated datasets (Fig. 4 in Tauxe et al., 2008), with the 95% confidence bounds on  $E$  value covering an interval from <1.5 to >3.0. So we think that the  $E/I$  method does detect some inclination shallowing but not its magnitude, the  $f = 0.6$  corresponding most probably to an upper limit of shallowing. So we use both original data and those

corrected for inclination shallowing for  $f = 0.6$  and regard both as proxies. Note also that the presence of shallowing is additional evidence for the primary origin of the HTC in the Zigan rocks.

Although polarity groups stand out, anomalous directions are present (Fig. 4a). In particular, note that the HTCs are reliably isolated from the samples with both “regular” (Fig. 3a–d) and anomalous directions (Fig. 3e–f). The HTCs were converted to virtual geomagnetic poles (VGP) and the overall mean pole was calculated. As is commonly adopted, any VGPs deviating by more than  $45^\circ$  from this pole were regarded as anomalous. For the data uncorrected for inclination shallowing, 17 anomalies are recognized. Ten anomalies fall between the neighboring N and R samples and are likely to be transitional directions, while the remaining seven may be either excursions or transitional directions close to missed polarity intervals. The ratio of anomalous directions to steady-field polarity ones is  $\sim 10\%$  before “unflattening”, and five more VGP’s became anomalous after it, thus increasing this ratio to  $\sim 12\%$ .

We found about 20 magnetozones within the about 80-meter thick section Z4, i.e. one reversal per  $\sim 4$  meters, of terrigenous redbeds of presumed molasse (Bekker, 1988). The reversals are even more frequent in sections Z1 and Z3 but the sections themselves are shorter and hence less statistically representative. In sum, there are 40 magnetozones (27 without single-sample horizons) in the  $\sim 110$  m thick combined section of the Zigan Fm.; the latter number gives the same four-meter interval between the reversals.

Multiple magnetozones in a small stratigraphic interval are not unique, but are typical in slowly deposited pelagic sediments (Gallet et al., 1992; Krystyn et al., 2002). In terrigenous sections, a similar number of magnetozones are known from sequences over a span of many hundred to several thousands of meters in thickness (e.g., Johnson et al., 1985; Gautam and Fujiwara, 2000; Gilder et al., 2001). Pavlov and Gallet (2001) found 28 polarity zones in an 850 m thick Middle Cambrian terrigenous sequence in NW Siberia and inferred the reversal frequency of  $6\text{--}8 \text{ RMa}^{-1}$ , which is about three times less than in the Zigan sections (Fig. 5). In the Siwaliks of Pakistan, Johnson et al. (1985) found 25 reversals in 1100 meters of red molasse sediments, that were correlated with high confidence to the Miocene reversal time scale and spanned 8 Myr. Therefore, about  $3 \text{ RMa}^{-1}$  are present in comparable sedimentary environments during a period of time known as the high reversal frequency Cenozoic interval. So, by comparison, the Zigan sections show extreme rates of magnetic reversals.

The same relatively high reversal rate is seen in other localities including Upper Ediacaran sediments ( $<560 \text{ Ma}$  to  $>540 \text{ Ma}$ ) in the White Sea region (Popov et al., 2005; Iglesia Llanos et al., 2005), where the reversal rate in short exposed sections looks very similar to our data (Fig. 6a). In the same area, 55 magnetozones are found in the  $\sim 400$  m long core of the Upper Ediacaran sequence in the Verkhotina borehole (Popov et al., 2005). Moreover, more than 20 more single-sample polarity intervals are found in this section. The fact that the distance between the adjacent sampling levels is only several meters indicates that the true number of reversals may be  $>80$ . For comparison, we present the polarity logs for two parts of the borehole core (Fig. 6b–c). Even if single-sample events are ignored, 12 polarity changes occur each 7–8 meters in the upper part of the core (Fig. 6b). For a wider interval of about 190 m (Fig. 6c), 24 magnetozones (without single-sample events) give a similar frequency of a reversal per 8 meters.

The second case of the very high reversal rate is from SW Siberia (Shatsillo et al., 2014, in press), where fifteen magnetozones are found in a  $\sim 45$ -meter thick redbeds of the Lopata Fm., which amounts to a reversal each  $\sim$  three meters. The authors of these data infer a Late Ediacaran–Early Cambrian age (555–540 Ma) for these rocks and estimate the duration of the studied section as ca. 1 Ma.

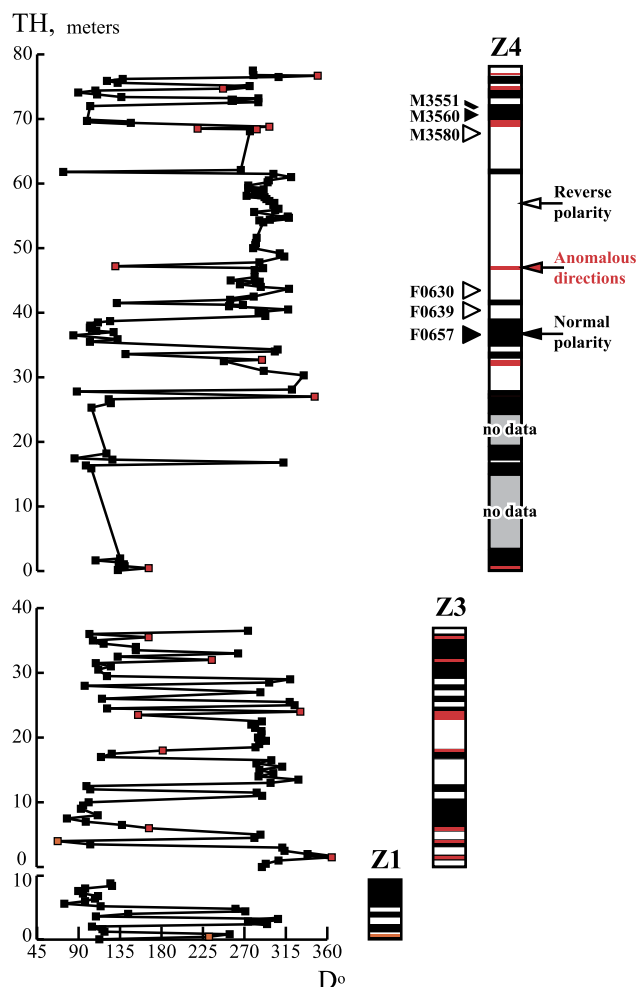
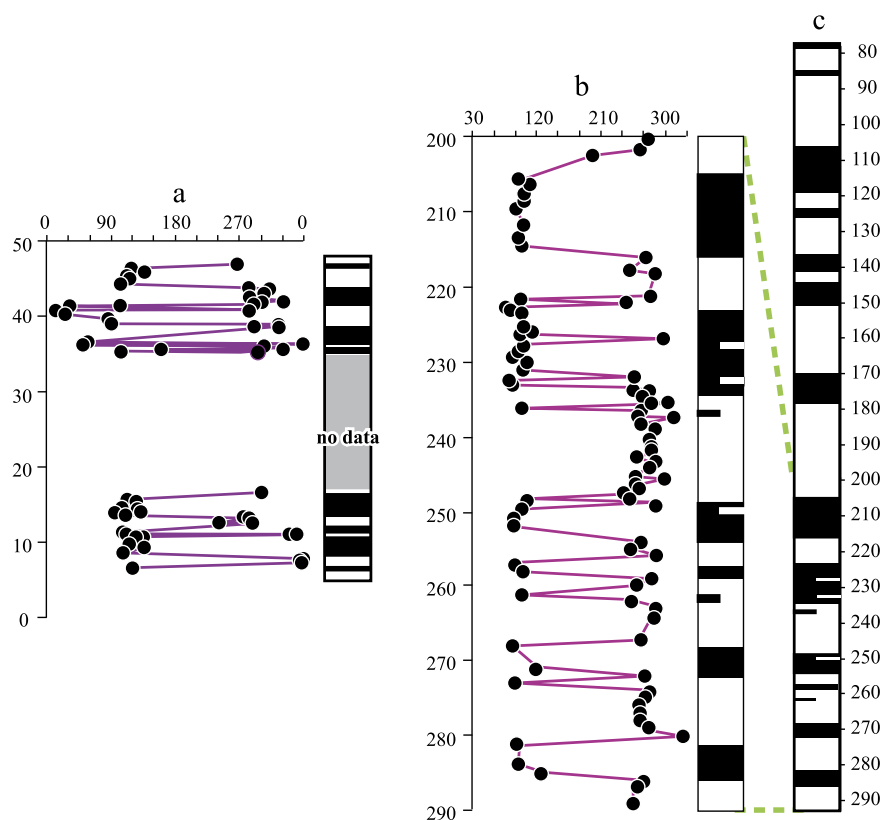


Fig. 5. Plots of declination ( $D^\circ$ ) versus thickness (TH, meters) for sections Z1, Z3, and Z4 and the corresponding polarity logs. Plots and logs are vertically spaced as suggested in Fig. 2b; thicknesses are given separately for each section. Normal, reversed, and anomalous data are shown by black, white and red intervals, respectively. Triangles on the left side indicate the thin-bed sites. (For interpretation of the references to color in this figure legend, the reader is referred to the web version of this article.)

Thus, in the Upper Ediacaran (ca.  $<560\text{--}>540 \text{ Ma}$ ) clastic sediments in three areas that are more than 2500 kilometers apart, the number of magnetozones is much larger, and their average thickness is much less, than in any other clastic section of any age.

#### 4. Origin of the ultra-high reversal rate

In principle, the observed ultra-high reversal rate (UHRR) may be attributed to subsequent remagnetization, although dual-polarity secondary components are relatively rare (e.g., Johnson and Van der Voo, 1989; Alexyutin et al., 2005). If a remagnetization model is invoked to explain the polarity pattern in the Zigan redbeds, it must simultaneously account for several related observations. Why have similar polarity patterns been met in the nearly coeval rock sequences from three areas more than 2500 kilometers apart, i.e., the NE coast of the White Sea, South Urals, and SW Siberia, but have never been found elsewhere in similar rocks of any other age? Of what age must this remagnetization be as the Zigan pole differs from all younger poles for Baltica? To our knowledge, no commonly invoked processes, like brine migration, chemical alteration, heating, etc., can result in acquisition of antipodal remanence directions on the few decimeters to few meters scale. Instead, the unique polarity pattern constitute a strong argu-



**Fig. 6.** Plots of declination ( $D^\circ$ ) versus thickness (TH, meters) and polarity logs for the White Sea area (simplified and modified after Popov et al., 2005). (a) Two short sections from exposures along the Zolotitsa River. (b) The Verkhotina borehole for the interval 200–290 m. (c) Polarity log for the interval 80–290 m. Note different vertical scale for these two polarity logs; green dashed lines show how they match. Note that the vertical scale in (a) and (b) is the same as in Fig. 5 to facilitate comparison. Other notation as in Fig. 5. (For interpretation of the references to color in this figure legend, the reader is referred to the web version of this article.)

ment in support of a primary remanence in Ediacaran rocks in the above three areas.

If the remanence origin cannot be challenged, can the UHRR be connected with unusually slow sedimentation rates at three remote localities at the nearly same time? The upper three formations of the Asha Series (Fig. 1c) were described as molasse (Bekker, 1988). Commonly, molasse have variable granulometry, from conglomerates to mudstones. The Asha rocks contain a single conglomerate horizon (the Kuk-Karauk Conglomerate Member). It is possible (and conservative) to argue that the Asha rocks accumulated in a distal part of a molasse basin on the passive margin of Baltica, either slightly above the sea level, or at a shallow depth, as evidenced by findings of Arumberia-type fossils (Kolesnikov et al., 2012). The White Sea area, where siliciclastic rocks accumulated in Ediacaran time (Sokolov and Fedonkin, 1985) and was a part of the stable craton several hundred kilometers inland from the Late Precambrian Timan orogen. Thus there is no clear reason to assume that sedimentation was many times slower in these two areas than anywhere else in the world with a comparable depositional setting.

Phanerozoic siliciclastic rocks, including redbeds, usually do not have abundant fossils, and fossil-based estimates of sedimentation rates are both rare and imprecise. So, even special volumes on clastic sedimentation appear to carefully avoid any quantitative estimates of these rates (e.g., Pettijohn et al., 1972), which is undoubtedly related to extreme variability of this parameter. Magnetostratigraphic data may give such estimates (e.g., Johnson et al., 1985; Gilder et al., 2001); note, however, that the reversal rate is best known for the Late Cretaceous–Cenozoic interval, with sedimentation rate varying from  $\sim 100$  m/Ma to  $>500$  m/Ma (Spencer, 1974; Kukal, 1983).

Additional age constraints are from the dated tuff that lies either within the lower part of the Zigan Formation (Levashova et al., 2013) or within the upper part of the Basu Formation (Kolesnikov et al., 2015); these two options are illustrated by stars in the general stratigraphic column (Fig. 1c). The stratigraphic problem is based primarily on two differing interpretations of the Ust-Katav stratigraphy where the Kuk-Karauk conglomerate (a diagnostic marker bed) is missing (Bekker, 1988; Levashova et al., 2013; Grazhdankin et al., 2011; Kolesnikov et al., 2015). Given this stratigraphic conundrum, we can calculate sedimentation rates by assuming (a) the 548 Ma age is from the upper Basu Formation or (b) the 548 Ma age is from the lower Zigan Formation. The most conservative estimate for sedimentation rate will be based on the assumption that the age is from the lower Zigan Formation.

Although Ediacaran fossils are problematic in their classification, there are several well-known constraints on their origins and extinctions in the fossil record. In particular, we note the end Kotlinian crisis ( $\sim 550$  Ma) where dickeniamorphs, rangeomorphs, tribrachiomorphs and bilateromorphs become extinct (Kolesnikov et al., 2015). The Asha Series contains numerous trace, macro and microfossils of Ediacaran affinity (Kolesnikov et al., 2015, and references therein). In particular, the uppermost Asha Series (Upper Zigan Formation) contains the first appearance of an ichnogenera closely resembling *Didymaulichnus* and none of the pre-Kotlinian genera. In the Olenek uplift of Siberia, strata containing the fossil *Didymaulichnus* are coeval with a tuff yielding a U–Pb age of  $543.9 \pm 0.3$  Ma (Bowring et al., 1993; Knoll et al., 1995). We use this age as the uppermost constraint on Asha Series deposition.

We calculate the most conservative sedimentation rates as follows using the measured sections given in Kolesnikov et al. (2015). If the 548 Ma age determination is from the Basu Fm., then  $\sim 800$  m of siliciclastic deposits were formed in 4–8 Ma (the 8 Ma



figure is using the maximum age error). The resultant sedimentation rate is 100–200 m/Ma. On the other hand, if the age determination is from the Zigan Formation, then ~450 m of siliclastics were deposited in 4–8 Ma. This conservative alternative yields a sedimentation rate between 60 and 110 m/Ma. These rates fall within the broad range for molasse deposits compiled by Spencer (1974) and Kukul (1983). In calculating our reversal rate, we use 80–100 m/Ma for the sedimentation rate in the Zigan.

## 5. The Ediacaran geomagnetic field

The reversal rate is known to vary widely over geologic time, dropping to zero during the superchrons (i.e. tens of million years) such as the Cretaceous Long Normal and Kiaman Reverse interval and attaining the level of 6–12 RMa<sup>-1</sup> in the Early-Middle Jurassic (Opdyke and Channell, 1996; Gradstein and Ogg, 2004; Biggin et al., 2012). If we use our estimate of sedimentation rate of 100 m/Ma (= 10 cm/ky), the reversal rate recorded in the Zigan Formation will be about 20–25 RMa<sup>-1</sup>. A sedimentation rate of <50 m/Ma (= 5 cm/ky) that has never been reported for continental clastic redbeds is required to reduce the observed reversal frequency to the Early-Middle Jurassic level that is still considered as an interval of UHRR. Thus we conclude that the existence of the UHRR is established robustly.

Establishing the time frame (i.e., the mean age and duration of the UHRR interval) is a different and more complicated matter. We should stress that frequent reversals were not reported from any Ediacaran rocks between 635 and 570 Ma (e.g., Schmidt and Williams, 2010), despite a rather large number of studies on terrigenous redbeds. In the White Sea region, a high to very high reversal rate is present in isolated outcrops (Fig. 6a) and, most importantly, the ~400 meter deep Verkhovina borehole (Popov et al., 2005). Unfortunately, the ties between the polarity log and the dated tuffs can only be deduced approximately. The oldest date of 558 ± 1 Ma in this area (Grazhdankin, 2003) is almost certainly older than the base of the polarity log in Popov et al. (2005), but there are no paleomagnetic data from this level. Two younger ages (552.85 ± 0.77 Ma (Martin et al., 2000; Schmitz, 2012) and 550.2 ± 4.6 Ma (Iglesia Llanos et al., 2005) are certainly within the polarity log, and, hence, a part of the UHRR is certainly younger than 550 Ma.

There are no reliable paleomagnetic data that may help to define the upper boundary of the UHRR. In Ediacaran sediments with ages <551 Ma in Podolia (Ukraine), the presence of six different components with overlapping distributions (Iosifidi et al., 2005) do not allow constructing a polarity log. The Nama Group in Namibia with the ages in ca. 550–540 Ma interval proved to have “a complex series of overprints and no easily discernible primary direction of magnetization” (Meert et al., 1997). We know of no commonly accepted magnetostratigraphic results of Lower Cambrian sedimentary successions. In fact, Kirschvink and Rozanov (1984) (also in Opdyke and Channell, 1996) claimed to find frequent reversals in the Lower Cambrian of East Siberia. Since then, the same sections and numerous other ones of similar age in Siberia have been studied and restudied, but the originally reported reversal pattern could not be reproduced (Pisarevsky et al., 1997; Torsvik et al., 1998; Gallet et al., 2003; Pavlov et al., 2004). In contrast, reliable paleomagnetic data from Middle Cambrian (ca. 510 Ma) sedimentary rocks in Siberia led Pavlov and Gallet (2001) and Gallet et al. (2003) to posit a high reversal rate of ~8 RMa<sup>-1</sup> albeit much lower than what we propose here.

Thus the entire UHRR interval could not last longer than from about 555 Ma until 510 Ma, but is likely to have been much shorter. Further narrowing this interval is hindered by several factors, including large ambiguities in regional correlation schemes, scarcity of isotopic ages on sedimentary sections both in Baltica

**Table 3**

Comparison of low-latitude paleomagnetic data on volcanics and the Zigan results.

#	Object	SLat	N	K	S°	Reference
1	Afar	11	41	25.3	16.3	Kidane et al., 2002
2	Costa Rica	10	30	22.7	17.2	Johnson et al., 2008
3	Ecuador	0	59	28.1	15.4	Opdyke et al., 2006
4	Kenya Mnt.	0	68	54.4	11.0	Opdyke et al., 2010
5	Loiyangalani	3	32	77.5	9.2	Opdyke et al., 2010
6	Yemen*	0	45	32.2	14.4	Riisager et al., 2005
7	Ethiopia*	0	57	22.5	17.2	Rochette et al., 1998
8	Zigan Fm.	8	(182)	17.4	19.6	This paper
9	Zigan Fm.**	12	(182)	13.1	22.7	This paper

Comments. #, result number. Slat, site latitude. N, the number of sites (samples) used. K, concentration parameter for VGPs, uncorrected for the within-site scatter. S, standard angular deviation for VGPs.

\* Paleolatitude instead of the present-day latitude is used.

\*\* Same dataset as #8 but corrected for inclination shallowing with  $f = 0.6$ .

and worldwide, our inability to date the purely sedimentary series. Both new magnetostratigraphic data and new radiometric ages are needed to better limit the UHRR duration. Our best estimate, is that the UHRR began sometime around 550 Ma and was in decay by the Middle Cambrian.

It has been suggested that the reversals would occur less frequently during periods when the ratio of the axial dipole field to the non-axial-dipole was larger on average (Cox, 1969). This model was further supported by computer simulations (Coe and Glatzmaier, 2006; see also Biggin et al., 2012). As shown above, the number of magnetozones is high in the Zigan sections, and the polarity mean directions are nearly antipodal. Based solely on our data, this test indicates that the Late Ediacaran geomagnetic field in its steady state was essentially zonal. Moreover, the agreement of the Zigan pole with the coeval data from the Middle Urals (Fedorova et al., 2014) and the White Sea region (Popov et al., 2005) indicates that the field was dipolar when not in the reversing state. Unfortunately, a lack of data on the field intensity in late Ediacaran time do not allow an assessment of the hypothesis that low dipole field strength correlates with high reversal rates (Biggin et al., 2012; Tauxe et al., 2013) although further work in this interval can provide a test of this hypothesis. At the same time, it's worth noting that the net field intensity in the Late Ediacaran has to be noticeably lower than during other epochs simply because the transitional intervals with lower-than-usual field intensity occupy a larger share of time.

There are no published estimates of the Ediacaran SV magnitude. We compare the Zigan results with available SV estimates (concentration parameter values,  $K$ , for VGPs) on thick volcanic series of different ages, as such SV estimates are considered as most reliable (Table 3; Fig. 7); this comparison is limited to the data from peri-equatorial regions. Unfortunately, there are only a few suitable datasets on volcanic rocks with the ages of <5 Ma (Table 3, #1–5) and just two on Oligocene lava piles (Table 3, #6–7). We compared both  $K$  values with other data with the aid of statistical  $F$ -test. With respect to the lowest  $K$  values for Cenozoic data (## 1–2, 7), the  $K$  value not corrected for shallowing for the Zigan dataset (#8) is marginally different, whereas the  $K$  value after correction (#9) is significantly less, albeit slightly so. A conservative conclusion is that the scatter (used as a proxy for SV magnitude) in the Zigan dataset is somewhat smaller than in the Cenozoic but the difference cannot be regarded as exceptionally large. Hence, the fastest ever reversal rate was not accompanied by clearly discernible change in the SV magnitude. Far more data is needed to fully test the notion that SV (and hence relative dipolar field strength) correlates directly with field strength by noting that our limited data make this distinction difficult (Biggin et al., 2012; Tauxe et al., 2013).

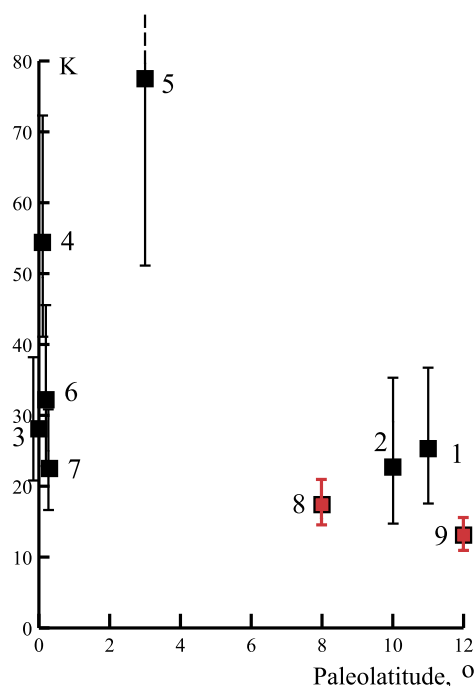


**Fig. 7.** Plot of concentration parameter  $K$  for VGPs versus latitude for the low-latitude data from peri-equatorial areas and the Late Ediacaran data from the Zigan Fm. (black and red squares, respectively). Vertical lines denote 95% confidence limits. Data are numbered as in Table 3. (For interpretation of the references to color in this figure legend, the reader is referred to the web version of this article.)

A common assumption is that a transitional interval between two polarity zones spans between 5 and 10 Ka (e.g., Merrill et al., 1996; Clement, 2004). If our adopted estimate of the reversal rate of  $20 \text{ RMa}^{-1}$  is correct, 10% to 20% of time should be represented by transitional fields. This estimate is in accord with the observed 10% to 12% share of anomalous directions in the Zigan data set (Fig. 4a), if all such directions are considered as transitional. In contrast, a recently posited transitional interval of  $\sim 1 \text{ ky}$  (Valet et al., 2012) would lead to a much smaller value of 1–2% of anomalous directions, in direct contrast to the observed data.

During the last two decades, extensive studies were dedicated to numerical simulations of geodynamo (e.g., Glatzmaier and Roberts, 1997; Christensen et al., 1998; Amit et al., 2010; Olson et al., 2011; Olson and Amit, 2014). Acknowledging the limited computational power required for these varied models, we note that it is difficult to compare our data directly with any particular field model. Nevertheless, we hope that future models might take into account the results described here in order to address the following questions: 1) Can the geomagnetic field reverse ca. 20 times during one Ma? 2) If yes, can the field preserve high axial symmetry and a 'typical' value of SV? 3) Is the UHRR a usual phenomenon or does it require some exceptional conditions? 4) Assuming our data truly reflect the field behavior in Late Ediacaran time along with previous published studies from the Cambrian, does the dipolar field 'decay' during this interval from a hyperactive state into a long-lived superchron?

## 6. Conclusions

A paleomagnetic study on Late Ediacaran sedimentary rocks showed that a high-temperature, dual-polarity component of demonstrably primary origin is present in the  $\sim 100$  meters thick section of the Upper Ediacaran clastic rocks in the western South Urals. The most intriguing feature of this dataset is the apparent very high reversal frequency, with consecutive reversals being sep-

arated by few decimeters to few meters and more than thirty polarity changes in total. This magnetostratigraphic pattern is unique for clastic rocks of any age and location, with a notable exception of roughly coeval Upper Ediacaran clastics from the SE part of the White Sea coast in Northern Russia and presumably coeval redbeds from SW Siberia. Analysis of available data shows that a remagnetization hypothesis for these rocks is difficult to argue and that the UHRR described herein is real. The duration of the UHRR is problematic as no reliable magnetostratigraphic data are available for the Early Cambrian. With strong reservations, the available data indicate that this UHRR existed between 570 Ma, which is an approximate age of the Basu Fm. in the South Urals with very modest reversal rate (Golovanova et al., 2011; Levashova et al., 2015), and 510 Ma, when "reasonably" high reversal frequency was found in the Middle Cambrian section in northwestern Siberia (Pavlov and Gallet, 2001).

Naturally, our finding of the frequently reversing and essentially dipolar (zonal) geomagnetic field with moderately high SV magnitude needs to be tested further. Hence a decisive test will be to discover the UHRR in sufficiently well dated rocks far away from Baltica. Moreover, if the duration of the UHRR is firmly established, this interval may serve as a marker for global correlation. The only obstacle is the lack of magnetostratigraphic data on Upper Ediacaran rocks. Perhaps, soon...

## Acknowledgements

We thank the people from Institute of Geology, the Ufimian Branch of Russian Academy of Sciences, who helped to carry out the fieldworks. Special thanks are due to Nina Dvorova and Olga Krezhovskikh for demagnetization and measurements of the collections. Detailed and instructive reviews by Lisa Tauxe, Mark Hounslow, Cornelis Langereis and an anonymous reviewer and comments by editor Gideon Henderson are sincerely appreciated. We thank Andrey Shatsillo, Nikolay Kuznetsov and Vladimir Pavlov for permission to use their submitted paper and subsequent heated debates. This study was funded by grants 12-05-00513 and 15-05-01860 (M. Bazhenov), 11-05-00037 (N. Levashova), and 11-05-00137 (I. Golovanova) from the Russian Foundation for Basic Research, Program #9, Earth Science Division, Russian Academy of Sciences, grant 14.Z50.31.0017 of the Government of the Russian Federation, and grant EAR11-19038 from the National Science Foundation (J. Meert). The conclusions in this paper reflect the views of the authors and not the funding agencies.

## References

- Alexyutin, M.V., Bachtadse, V., Alexeev, D.V., Nikitina, O.I., 2005. Paleomagnetism of Ordovician and Silurian rocks from the Chu-Yili and Kandyktas mountains, South Kazakhstan. *Geophys. J. Int.* 162, 321–331.
- Amit, H., Leonhardt, R., Wicht, J., 2010. Polarity reversals from paleomagnetic observations and numerical dynamo simulations. *Space Sci. Rev.* 155, 293–335.
- Bekker, Y.R., 1988. Precambrian Molasses. Nedra, Leningrad. 289 pp. (in Russian).
- Biggin, A.J., Steinberger, B., Aubert, J., Suttie, N., Holme, R., Torsvik, T.H., van der Meer, D.G., van Hinsbergen, D.J.J., 2012. Possible links between long-term geomagnetic variations and whole-mantle convection processes. *Nat. Geosci.* 5, 526–533.
- Bowring, S.A., Grotzinger, J.P., Isachsen, C.E., Knoll, A.H., Pelechaty, S.M., Kolosov, P., 1993. Calibrating rates of Early Cambrian evolution. *Science* 261, 1293–1298.
- Brown, D., Spadea, P., Puchkov, V., Alvarez-Marron, J., Herrington, R., Willner, A.P., Hetzel, R., Gorozhanina, Y., Juhlin, C., 2006. Arc-continent collision in the Southern Urals. *Earth-Sci. Rev.* 79 (3–4), 261–287.
- Christensen, U., Olson, P., Glatzmaier, G., 1998. A dynamo model interpretation of geomagnetic field structures. *Geophys. Res. Lett.* 25, 1565–1568.
- Clement, B.M., 2004. Dependence of the duration of geomagnetic polarity reversals on site latitude. *Nature* 428, 637–640.
- Coe, R.S., Glatzmaier, G.A., 2006. Symmetry and stability of the geomagnetic field. *Geophys. Res. Lett.* 33, L21311. <http://dx.doi.org/10.1029/2006GL027903>.
- Cogné, J.P., 2003. PaleoMac: a Macintosh application for treating paleomagnetic data and making plate reconstructions. *Geochem. Geophys. Geosyst.* 4 (1), 1007. <http://dx.doi.org/10.1029/2001GC000227>.

- Cox, A., 1969. Geomagnetic reversals. *Science* 163, 237–245.
- Fedorova, N.M., Levashova, N.M., Meert, J.G., Maslov, A.V., Krupenin, M.T., 2014. New paleomagnetic data on Baltica based on Upper Ediacaran deposits on the Western Slope of the Middle Urals. *Dokl. Earth Sci.* 456, 512–516.
- Fisher, R.A., 1953. Dispersion on a sphere. *Proc. R. Soc. London, Ser. A* 217, 295–305.
- Gallet, Y., Besse, J., Krystyn, L., Marcoux, J., Theveniaut, H., 1992. Magnetostratigraphy of the Late Triassic Boluçekasi Tepe section (southwestern Turkey): implications for changes in magnetic reversal frequency. *Phys. Earth Planet. Inter.* 73, 85–108.
- Gallet, Y., Pavlov, V., Courtillot, V., 2003. Magnetic reversal frequency and apparent polar wander of the Siberian platform in the earliest Palaeozoic, inferred from the Khorbusuonka river section (northeastern Siberia). *Geophys. J. Int.* 154, 829–840.
- Gautam, P., Fujiwara, Y., 2000. Magnetic polarity stratigraphy of Siwalik Group sediments of Karnali River section in western Nepal. *Geophys. J. Int.* 142 (3), 812–824.
- Gilder, S., Chen, Y., Sen, S., 2001. Oligo-Miocene magnetostratigraphy and rock magnetism of the Xishuigou section, Subei (Gansu Province, western China) and implications for shallow inclinations in central Asia. *J. Geophys. Res.* 106, 30,505–30,521.
- Glatzmaier, G.A., Roberts, P.H., 1997. Simulating the geodynamo. *Contemp. Phys.* 38, 269–288.
- Golovanova, I.V., Danukalov, K.N., Kozlov, V.I., Puchkov, V.N., Pavlov, V.E., Gallet, Y., Levashova, N.M., Sirota, G.S., Khairullin, R.R., Bazhenov, M.L., 2011. Paleomagnetism of the upper Vendian Basu Formation of the Bashkirian Meganticlinorium revisited. *Izv. Phys. Solid Earth* 47, 623–635.
- Gradstein, F.M., Ogg, J.G., 2004. Geologic time scale 2004 – why, how, and where next! *Lethaia* 37, 175–181.
- Grazhdankin, D.V., 2003. The composition and depositional environment of the Vendian complex in the Southeastern White Sea region. *Stratigr. Geol. Correl.* 11 (4), 3–34.
- Grazhdankin, D.V., Marusin, V.V., Meert, J., Krupenin, M.T., Maslov, A.V., 2011. Kotlin regional stage in the South Urals. *Dokl. Earth Sci.* 440, 1222–1226.
- Grazhdankin, D.V., 2014. Patterns of evolution of the Ediacaran soft-bodied biota. *J. Paleontol.* 88, 269–283.
- Iglesia Llanos, M.P., Tait, J.A., Popov, V., Abalmassova, A., 2005. Paleomagnetic data from Ediacaran (Vendian) sediments of the Arkhangelsk region, NW Russia: an alternative apparent polar wander path of Baltica for the Late Proterozoic–Early Palaeozoic. *Earth Planet. Sci. Lett.* 240, 732–747.
- Iosifidi, A.G., Khramov, A.N., Bachtadse, V., 2005. Multicomponent magnetization of Vendian sedimentary rocks in Podolia, Ukraine. *Rus. J. Earth Sci.* 7 (1), 1–14.
- Johnson, C.L., Constable, C.G., Tauxe, L., Barendregt, R.W., Brown, L.L., Coe, R.S., Layer, P.W., Mejia, V., Opdyke, N.D., Singer, B.S., Staudigel, H., Stone, D.B., 2008. Recent investigations of the 0- to 5-Ma geomagnetic field recorded by lava flows. *Geochem. Geophys. Geosyst.* 9, Q04032. <http://dx.doi.org/10.1029/2007GC001696>.
- Johnson, N.M., Stix, J., Tauxe, L., Cervený, P.F., Tahirkheli, R., 1985. Paleomagnetic chronology, fluvial processes, and tectonic implications of the Siwalik deposits near Chinji village, Pakistan. *J. Geol.* 93, 27–40.
- Johnson, R.J.E., Van der Voo, R., 1989. Dual-polarity early Carboniferous remagnetization of the Fisset Brook Formation, Cape Breton Island, Nova-Scotia. *Geophys. J. (Oxf.)* 97, 259–273.
- Keller, B.M., Chumakov, N.M. (Eds.), 1983. *Stratotype of the Riphean: Stratigraphy, Geochronology*. Nauka, Moscow, 184 pp. (in Russian).
- Kidane, T., Abebe, B., Courtillot, V., Herrero, E., 2002. New paleomagnetic result from the Ethiopian flood basalts in the Abbay (Blue Nile) and Kessam gorges. *Earth Planet. Sci. Lett.* 203, 353–367.
- Kirschvink, J.L., 1980. The least-square line and plane and the analysis of palaeomagnetic data. *Geophys. J. R. Astron. Soc.* 62, 699–718.
- Kirschvink, J.L., Rozanov, A.Y., 1984. Magnetostratigraphy of Lower Cambrian strata from the Siberian Platform: palaeomagnetic pole and preliminary polarity time-scale. *Geol. Mag.* 121 (3), 189–203.
- Knoll, A.H., Grotzinger, J.P., Kaufman, A.J., Kolosov, P., 1995. Integrated approaches to terminal Proterozoic stratigraphy: an example from the Olenek Uplift, north-eastern Siberia. *Precambrian Res.* 73, 251–270.
- Kolesnikov, A.V., Grazhdankin, D.V., Maslov, A.V., 2012. Arumberia-type structures in the Upper Vendian of the Urals. *Dokl. Earth Sci.* 447, 1233–1239.
- Kolesnikov, A.V., Marusin, V.V., Nagovitsin, K.E., Maslov, A.V., Grazhdankin, D.V., 2015. Ediacaran biota in the aftermath of the Kotlinian Crisis: Asha Group of the South Urals. *Precambrian Res.* 263, 59–78.
- Kozlov, V.I. (Ed.), 2002. *Geological Map of the Russian Federation and Adjacent Territory of the Republic of Kazakhstan. Scale: 1:1 000 000 (a New Series). Sheet N-40(41)-Ufa*. VSEGEI, St. Petersburg.
- Krystyn, L., Gallet, Y., Besse, J., Marcoux, J., 2002. Integrated Upper Carnian to Lower Norian biochronology and implications for the Upper Triassic magnetic polarity time scale. *Earth Planet. Sci. Lett.* 203, 343–351.
- Kukal, Z., 1983. *The Rates of Geologic Processes*. Academia, Praha, 246 pp.
- Kuznetsov, N.B., Romanyuk, T.V., Shatsillo, A.V., Golovanova, I.V., Danukalov, K.N., Meert, J.G., 2012. The first results of mass isotope dating (LA-ICP-MS) for detrital zircons from the Asha Group, South Urals: paleogeography and paleotectonics. *Dokl. Earth Sci.* 447, 1240–1246.
- Kuznetsov, N.B., Meert, J.G., Romanyuk, T.V., 2014. Ages of detrital zircons (U/Pb, LA-ICP-MS) from the Latest Neoproterozoic–Middle Cambrian (?) Asha Group and Early Devonian Takaty Formation, the Southwestern Urals: a test of an Australia–Baltica connection within Rodinia. *Precambrian Res.* 244, 288–305.
- Levashova, N.M., Bazhenov, M.L., Meert, J.G., Kuznetsov, N.B., Golovanova, I.V., Danukalov, K.N., Fedorova, N.M., 2013. Paleogeography of Baltica in the Ediacaran: paleomagnetic and geochronological data from the clastic Zigan Formation, South Urals. *Precambrian Res.* 236, 16–30.
- Levashova, N.M., Bazhenov, M.L., Meert, J.G., Danukalov, I.V., Golovanova, N.B., Kuznetsov, K.N., Fedorova, N.M., 2015. Paleomagnetism of upper Ediacaran clastics from the South Urals: implications to paleogeography of Baltica and the opening of the Iapetus ocean. *Gondwana Res.* 28, 191–208.
- Martin, M.W., Grazhdankin, D.V., Bowring, S.A., Evans, D.A.D., Fedonkin, M.A., Kirschvink, J.L., 2000. Age of Neoproterozoic bilaterian body and trace fossils, White Sea, Russia: implications for metazoan evolution. *Science* 288, 841–845.
- McFadden, P.L., McElhinny, M.W., 1990. Classification of the reversal test in paleomagnetism. *Geophys. J. Int.* 103, 725–729.
- Meert, J.G., Eide, E.A., Torsvik, T.H., 1997. The Nama Group revisited. *Geophys. J. Int.* 129, 637–650.
- Merrill, R.T., McElhinny, M.W., McFadden, P.L., 1996. *The Magnetic Field of the Earth*. Acad. Press, San Diego, 527 pp.
- Olson, P.L., Glatzmaier, G.A., Coe, R.S., 2011. Complex polarity reversals in a geodynamo model. *Earth Planet. Sci. Lett.* 304, 168–179.
- Olson, P., Amit, H., 2014. Magnetic reversal frequency scaling in dynamos with thermochemical convection. *Phys. Earth Planet. Inter.* 229, 122–133.
- Opdyke, N.D., Channell, J.E.T., 1996. *Magnetic Stratigraphy*. Int. Geophys. Ser., vol. 64. Academic Press, London, New York, 346 pp.
- Opdyke, N.D., Hall, M., Mejia, V., Huang, K., Foster, D.A., 2006. Time-averaged field at the equator: results from Ecuador. *Geochem. Geophys. Geosyst.* 7, Q11005. <http://dx.doi.org/10.1029/2005GC001221>.
- Opdyke, N.D., Kent, D.V., Huang, K., Foster, D.A., Patel, J.P., 2010. Equatorial paleomagnetic time-averaged field results from 0–5 Ma lavas from Kenya and the latitudinal variation of angular dispersion. *Geochem. Geophys. Geosyst.* 11, Q05005. <http://dx.doi.org/10.1029/2009GC002863>.
- Pavlov, V.E., Gallet, Y., 2001. Middle Cambrian high magnetic reversal frequency (Kulumbé River section, northwestern Siberia) and reversal behavior during the Early Palaeozoic. *Earth Planet. Sci. Lett.* 185, 173–183.
- Pavlov, V., Gallet, Y., Shatsillo, A., Vodovozov, V., 2004. Paleomagnetism of the Lower Cambrian from the Lower Lena River Valley: constraints on the apparent polar wander path from the Siberian platform and the anomalous behavior of the geomagnetic field at the beginning of the Phanerozoic. *Izv. Phys. Solid Earth* 40, 114–133.
- Pavlov, V.E., Gallet, Y., 2005. A third superchron during the Early Paleozoic. *Episodes* 28 (2), 78–84.
- Pavlov, V., Gallet, Y., 2010. Variations in geomagnetic reversal frequency during the Earth's middle age. *Geochem. Geophys. Geosyst.* 11, Q01210. <http://dx.doi.org/10.1029/2009GC002583>.
- Pettijohn, F.J., Potter, P.E., Siever, R., 1972. *Sand and Sandstone*. Springer-Verlag, Berlin, 535 pp.
- Pisarevsky, S.A., Gurevich, E.L., Khramov, A.N., 1997. Paleomagnetism of Lower Cambrian sediments from the Olenek river section (northern Siberia): paleopoles and the problem of magnetic polarity in the Early Cambrian. *Geophys. J. Int.* 130, 746–756.
- Popov, V., Iosifidi, A., Khramov, A., Tait, J., Bachtadse, V., 2002. Paleomagnetism of Upper Vendian sediments from the Winter Coast, White Sea region, Russia: implications for the paleogeography of Baltica during Neoproterozoic times. *J. Geophys. Res.* 107. <http://dx.doi.org/10.1029/2001JB001607>.
- Popov, V.V., Khramov, A.N., Bachtadse, V., 2005. Paleomagnetism, magnetic stratigraphy, and petromagnetism of the Upper Vendian sedimentary rocks in the sections of the Zolotitsa River and in the Verkhotina Hole, Winter Coast of the White Sea, Russia. *Rus. J. Earth Sci.* 7 (2), 1–29.
- Puchkov, V.N., 1997. Structure and Geodynamics of the Uralian Orogen. *Geological Society Special Publication*, vol. 121, pp. 201–236.
- Puchkov, V.N., 2003. The Uralides and Timanides: their structural relationship and position in the geologic history of the Ural–Mongolian fold belt. *Russ. Geol. Geophys.* 44 (1–2), 28–39.
- Riisager, P., Knight, K.B., Baker, J.A., Peate, I.U., Al-Kadasi, M., Al-Subbar, A., Renne, P.R., 2005. Paleomagnetism and  $^{40}\text{Ar}/^{39}\text{Ar}$  Geochronology of Yemeni Oligocene volcanics: implications for timing and duration of Afro-Arabian traps and geometry of the Oligocene paleomagnetic field. *Earth Planet. Sci. Lett.* 237, 647–672.
- Rochette, P., Tamrat, E., Feraud, G., Pik, R., Courtillot, V., Ketefo, E., Coulon, C., Hoffmann, C., Vandamme, D., Yigru, G., 1998. Magnetostratigraphy and timing of the Oligocene Ethiopian traps. *Earth Planet. Sci. Lett.* 164, 497–510.
- Schmidt, P.W., Williams, G.E., 2010. Ediacaran paleomagnetism and apparent polar wander path for Australia: no large true polar wander. *Geophys. J. Int.* 182, 711–726.
- Schmitz, M.D., 2012. Appendix 2—Radiometric ages used in GTS2012. In: Gradstein, F., Ogg, J., Schmitz, M.D., Ogg, G. (Eds.), *The Geologic Time Scale 2012*. Elsevier, Boston, pp. 1045–1082.
- Shatsillo, A.V., Kuznetsov, N.B., Pavlov, V.E., 2014. First paleomagnetic data on the stratotype section of the Lopata Formation, the Teya–Chapa basin (Yenisei

- Ridge): implications to the age of the terminal Precambrian in the region. In: *Proceedings of Scientific Meeting "Geodynamic Evolution of the Lithosphere in the Central Asia"*, IZK SB RAS, Irkutsk, pp. 331–332 (in Russian).
- Shatsillo, A.V., Kuznetsov, N.B., Fedonkin, M.A., Priyatkina, N.S., Serov, S.G., in press. First magnetostratigraphic data for the stratotype of the Upper Neoproterozoic Lopata Formation (the north-east Yenisei Ridge): problems of its age and paleogeography of the Siberian Platform at the boundary of the Phanerozoic and Proterozoic. *Dokl. Earth Sci.*, 2015.
- Sokolov, B.S., Fedonkin, M.A. (Eds.), 1985. *The Vendian System*, vol. 2. Nauka, Moscow, 239 pp. (in Russian).
- Spencer, E.M. (Ed.), 1974. *Mesozoic–Cenozoic Orogenic Belts. Data for Orogenic Studies*, Geological Society London. Scottish Academic Press, Edinburgh. 809 pp.
- Tauxe, L., Kent, D.V., 2004. A simplified statistical model for the geomagnetic field and the detection of shallow bias in Paleomagnetic inclinations: was the ancient magnetic field dipolar? In: Channell, J.E.T., Kent, D.V., Lowrie, W., Meert, J.G. (Eds.), *Timescales of the Paleomagnetic Field*. In: *AGU Geophys. Monogr.*, vol. 135, pp. 101–116.
- Tauxe, L., Kodama, K.P., Kent, D.V., 2008. Testing corrections for paleomagnetic inclination error in sedimentary rocks: a comparative approach. *Phys. Earth Planet. Inter.* 169, 152–165.
- Tauxe, L., Gee, J.S., Steiner, M.B., Staudigel, H., 2013. Paleointensity results from the Jurassic: new constraints from submarine basaltic glasses of ODP Site 801C. *Geochem. Geophys. Geosyst.* 14, 4718–4733.
- Torsvik, T.H., Meert, J.G., Smethurst, M.A., 1998. Polar wander and the Cambrian. *Science* 279 (5349), 307.
- Torsvik, T.H., Van der Voo, R., Preeden, U., Mac Niocaill, C., Steinberger, B., Doubrovine, P.V., van Hinsbergen, D.J.J., Domeier, M., Gaina, C., Tohver, E., Meert, J.G., McCausland, P.J.A., Cocks, L.R.M., 2012. Phanerozoic polar wander, palaeogeography and dynamics. *Earth-Sci. Rev.* 114, 325–368.
- Valet, J.-P., Fournier, A., Courtillot, V., Herrero-Bervera, E., 2012. Dynamical similarity of geomagnetic field reversals. *Nat. Geosci.* 49, 89–94.
- Zijderveld, J.D.A., 1967. AC demagnetization of rocks: analysis of results. In: Collinson, D.W., Creer, K.M. (Eds.), *Methods in Paleomagnetism*. Elsevier, Amsterdam, pp. 254–286.